ZEKE electron spectroscopy of alkylbenzene–argon van der Waals complexes

ARTICLE *in* JOURNAL OF ELECTRON SPECTROSCOPY AND RELATED PHENOMENA · NOVEMBER 2000

Impact Factor: 1.44 · DOI: 10.1016/S0368-2048(00)00218-8

6 AUTHORS, INCLUDING:

Shin-ichiro Sato
Hokkaido University
107 PUBLICATIONS **1,082** CITATIONS
SEE PROFILE

Hidenori Shinohara
TDK Corporation
15 PUBLICATIONS **153** CITATIONS
SEE PROFILE

ELSEVIER

Journal of Electron Spectroscopy and Related Phenomena 112 (2000) 247–255

JOURNAL OF ELECTRON SPECTROSCOPY and Related Phenomena

www.elsevier.nl/locate/elspec

ZEKE electron spectroscopy of alkylbenzene–argon van der Waals complexes

S. Sato[a,b,*], T. Kojima[a], K. Byodo[a], H. Shinohara[a], S. Yanagihara[a], K. Kimura[1]

[a]*School of Materials Science, Japan Advanced Institute of Science and Technology, Tatsunokuchi 923-1292, Japan*
[b]*Department of Molecular Chemistry, Graduate School of Engineering, Hokkaido University, Sapporo 060-8628, Japan*

Received 18 April 2000; accepted 15 July 2000

Abstract

Van der Waals (vdW) complexes of a series of alkylbenzenes (benzene, toluene, ethylbenzene, and n-propylbenzene) formed with Ar in supersonic jets have been studied with two-color zero-kinetic-energy (ZEKE) electron spectroscopy combined with a PFI (pulsed field ionization) method. The shifts in adiabatic ionization energies (I_a) due to complex formation have been determined as -128 and -112 cm^{-1} for ethylbenzene–Ar and n-propylbenzene–Ar, respectively, with respect to the bare molecules. These shifts have been reproduced qualitatively in terms of atom–atom Lennard–Jones (LJ) potentials incorporating charge–charge-induced-dipole interactions. Some low-frequency ZEKE bands due to vdW vibrations have been observed for benzene–Ar for the first time. However, no vdW vibrational structures appear in ZEKE electron spectra both for ethylbenzene–Ar and n-propylbenzene–Ar. The absence of vdW vibrational structure in the spectra may be probably due to a steric hindrance between Ar and the alkyl group. This has been supported also by the present LJ potential calculations. Furthermore, for toluene–Ar, it has been found that upon ionization the relative position of Ar is shifted along the direction of the C–C(H_3) bond.

Keywords: Alkylbenzenes; Ar vdW complexes; ZEKE electron spectra; Lennard-Jones

1. Introduction

Molecular van der Waals (vdW) complexes produced in supersonic jets have attracted much interest in physical chemistry for many years, because of their low binding energies, large intermolecular equilibrium distances, and very low frequency vdW vibrations. Very recently, Kimura [1] has published an extensive review article on the studies of jet-cooled aromatic–argon van der Waals molecules by two-color ZEKE (zero kinetic energy) electron spectroscopy.

Laser photoelectron spectroscopy based on one- or two-color REMPI (resonantly enhanced multiphoton ionization) with a pulsed UV/Visible lasers has been developed to study not only neutral excited-state molecules but also their cationic states from photoelectron kinetic energy spectra [2,3]. The first example studied by this technique for a molecular vdW

*Corresponding author. Tel.: +81-11-706-6607; fax: +81-11-709-2037.
E-mail addresses: s-sato@eng.hokudai.ac.jp (S. Sato), k-kimura@crl.go.jp (K. Kimura).
[1]Present address: Molecular Photonics and Photoelectron Group, National Communications Research Laboratory, Shidami Science Park, 2268-1 Anagahora, Nagoya 463-0003, Japan.

0368-2048/00/$ – see front matter
PII: S0368-2048(00)00218-8

complex is the NO–Ar vdW complex produced in a jet [4].

The REMPI-based photoelectron technique was soon extended to two-color ZEKE electron spectroscopy, which has been developed by Schlag and co-workers [5–7] and also by Kimura and co-workers [8–13], providing a powerful tool for carrying out cation spectroscopy for a molecular species in very high resolution. Experimentally a jet-cooled molecular species is first excited by the first laser to a specific resonant excited state, and further excited by the second laser to a high-lying Rydberg level from which a ZEKE electron is detected. For aromatic molecules, the lowest singlet excited state (S_1) is usually selected as a resonant excited state in such two-color experiments. A two-color ZEKE electron technique has an excellent state- and species-selectivity for a mixture of various molecular species. A compact high-brightness cm^{-1}-resolution ZEKE electron analyzer with a short flight distance has been earlier developed by Kimura and colleagues [9–11], and it has been later combined with a two-pulsed field ionization technique [14].

The characteristics of two-color (1+1′) ZEKE electron spectroscopy in studying vdW complexes are the following: (1) a specific vdW complex can be selected from a mixture of jet-cooled analogous species by tuning the first pulsed laser to an appropriate resonant excited state; (2) the excited-state vdW complex thus selected is further excited by the second pulsed laser to a high-lying Rydberg state just several wavenumbers below an ionization threshold; (3) ZEKE electrons can be detected as a function of the second laser wavelength by applying a delayed pulsed electric field. The energy axis of ZEKE electron spectrum therefore can be determined in a resolution of the laser wavelength.

Using a ZEKE electron technique, Chewter et al. [6] have observed the cation origin band for the benzene–Ar vdW complex that is shifted by 172 cm^{-1} with respect to the bare benzene. The observation of cation vdW vibrations by ZEKE electron spectroscopy has been reported first for NO–Ar [11,12] and also for aniline–Ar_n ($n=1$ and 2) [13,15]. Since then, a number of studies of cation spectroscopy for aromatic vdW complexes have been carried out, mainly by ZEKE photoelectron spectroscopy [1].

The van der Waals (vdW) complexes of an organic aromatic molecule with rare gas atoms are expected to provide basic information on the structural, energetic, and dynamic manifestations of intermolecular interactions in well-characterized chemical systems. The adiabatic ionization potentials (I_a) of various aromatic molecules are lowered in general upon complex formation with rare gas atoms [6,13,15–27]. For example, the benzene–Ar complex gives a lowering of $\Delta I_a=172$ cm^{-1} [6], while the toluene–Ar complex gives a lowering of $\Delta I_a=166$ cm^{-1} [18,25]. It is noted that recent development of ZEKE electron spectroscopy makes it possible to study the I_a lowerings in detail for various vdW complexes.

For the benzene–Ar and toluene–Ar vdW complexes, their S_1 origins have been earlier studied with LIF (laser induced fluorescence) spectroscopy [28]. For ethylbenzene–Ar and *trans* n-propylbenzene–Ar, their S_1 origins have been determined in the present study with time-of-flight (TOF) mass multiphoton ionization (MPI) excitation spectroscopy.

The lowering in I_a upon the complex formation of an aromatic molecule with Ar may be explained qualitatively as an addition of charge–charge-induced-dipole interaction. The small difference in the lowering of I_a between benzene–Ar (172 cm^{-1}) and toluene–Ar (166 cm^{-1}) addressed us to extend our study to a series of vdW complexes with higher alkylbenzenes. In the present study we also carried out semi-quantitative Lennard–Jones (LJ) calculations including charge–charge-induced-dipole interaction to interpret the observed lowerings in I_a for the vdW complexes of the alkylbenzenes with Ar.

The atom–atom LJ potential parameters of neutral organic aromatic molecules with rare gas atoms have well been determined by Leutwyler and Jortner [29]. In our previous ZEKE electron spectroscopic study of azulene–Ar [27], we have performed theoretical calculations of LJ potentials including charge–charge-induced-dipole interactions, and found that the observed lowering in I_a as well as the vdW bending frequency can be well reproduced semi-quantitatively.

2. Experimental

A two-color ZEKE and TOF-MPI apparatus used in the present study is essentially the same as that

previously described [14]. The development of our REMPI-based photoelectron apparatus and several kinds of two-color ZEKE electron analyzers have recently been described in detail in a review article by Kimura [30]. A two-pulsed-field ionization technique previously developed in this laboratory [14] was used in the present experiments, schematically shown in Fig. 1, together with a timing chart of the two pulsed electric fields in relation to the second laser shot. Two tunable dye lasers pumped by a nanosecond Nd:YAG laser (10 Hz repetition) were used in the present two-color experiments.

Prior to our ZEKE electron measurements, one-color TOF-MPI excitation spectra were recorded to determine the S_1 origins of the vdW complexes studied, which were excited into the S_1 manifold and simultaneously ionized with the same laser. The ions thus produced were mass-separated by a TOF mass analyzer of 20-cm long, and one-color TOF-MPI spectra were measured as a function of the laser wavelength.

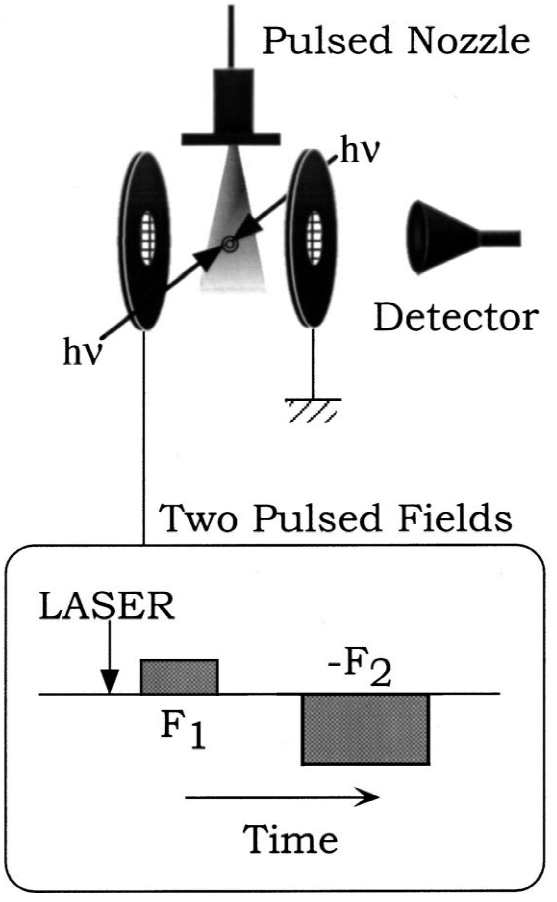

Fig. 1. A schematic drawing of a 'two-pulsed field ionization' ZEKE electron analyzer and a timing chart of the pulsed electric fields in relation to the second laser shot. The discrimination field ($+F_1$) and the collection field ($-F_2$) are also indicated.

In two-color ZEKE electron measurements, the molecular species studied were excited by the first laser to the S_1 origin already determined from the TOF-MPI spectra, and then further excited by the second laser to high-lying Rydberg states within a few wavenumbers below the ionization threshold. Briefly, 50 ns after the laser shot, a positive pulsed electric field ($+F_1$) was first applied for 200 ns to remove energetic electrons as well as threshold electrons. After a delay of 700 ns, a negative electric field ($-F_2$) was applied for 1 μs to ionize deeper Rydberg states as ZEKE electrons. ZEKE electron spectra were measured as a function of the second excitation laser wavelength. The peak positions were determined by an interferometer (Buleigh WA-5500) within an accuracy of ± 6 cm^{-1}.

A sample of aromatic molecules is mixed with Ar, and expanded into a vacuum chamber through a pulsed nozzle at a typical stagnation pressure of 1–4 Atm. The background pressure in the chamber was maintained at $1–2\times10^{-5}$ Torr during our measurements.

3. Results and discussion

3.1. Isomers of ethylbenzene–Ar and n-propylbenzene–Ar (trans)

There are two possible conformers (orthogonal and planar) in ethylbenzene and *trans* n-propylbenzene, though these conformers are absent in benzene and toluene. Studies of ethylbenzene by microwave spectroscopy [31] and ab initio calculations [31,32] have indicated that the orthogonal form is more stable than the planar form. Fig. 2 displays the potential energy surfaces of the ethyl group of ethylbenzene at the neutral (S_0) and cation (D_0) states. These potential curves were obtained from our ab initio calculations with the Beck's three-parameter hybrid density functional method (B3LYP) [33] using the Gaussian 94 program package [34] on the basis of the 6-31G* basis set. No potential well was

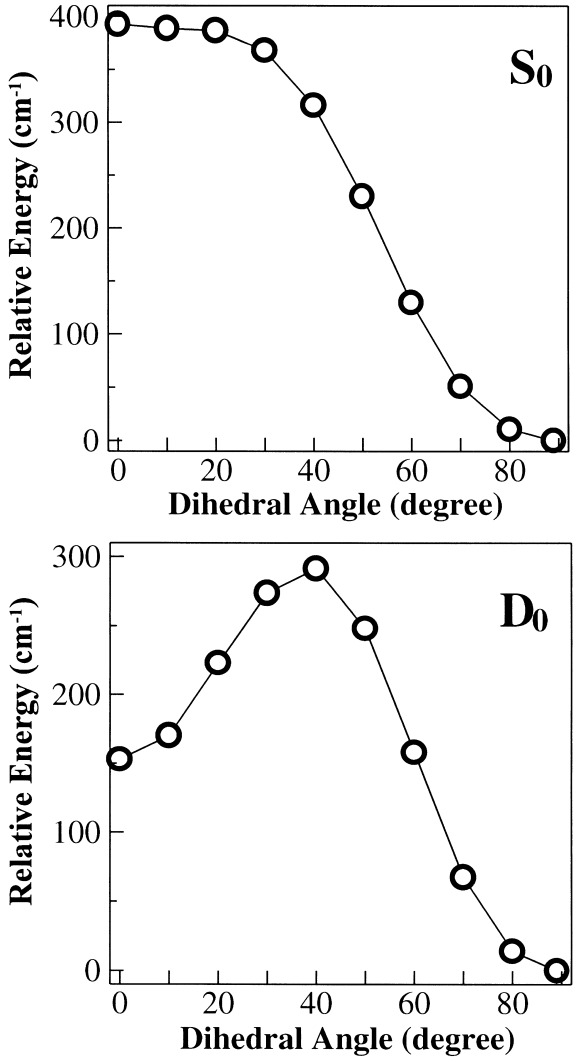

Fig. 2. Potential energy curves of ethylbenzene both at the neutral ground state (S_0) and at the cation ground state (D_0), plotted against the dihedral angle of the ethyl group with respect to the phenyl plane. Geometrical parameters other than the dihedral angle were fully optimized at each calculated point.

observed for the neutral ethylbenzene in the planar form, as revealed in the previous studies [31], so that the neutral ethylbenzene may take the orthogonal form. From our calculations it has been found that there should be a stable conformer with a planar structure at the cationic state.

The orthogonal form provides two different cites to which the Ar atom attaches, leading to two

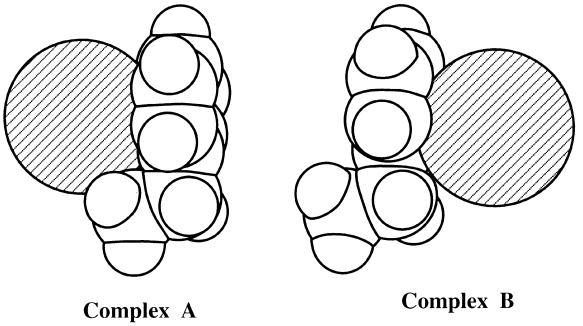

Fig. 3. Two possible isomers (A and B) for the ethylbenzene–Ar vdW complex.

isomers A and B for ethylbenzene, as shown schematically in Fig. 3. The Ar atom in isomer A is attached to the phenyl plane to which the ethyl group is tilted, while in isomer B the Ar atom is attached to the opposite site. Ab initio full geometry optimizations were carried out for the two isomers (A and B) of ethylbenzene–Ar, using the RHF-MP2/3-21^{+}G** method. The rotational constants of ethylbenzene–Ar are summarized in Table 1, obtained from the optimized structures. The bare ethylbenzene is approximated as a symmetric top molecule. The isomer A of ethylbenzene–Ar is also well approximated as a symmetric top molecule, but the isomer B is not.

3.2. MPI excitation spectra

Fig. 4 shows rotational contours observed in TOF-MPI excitation spectra at around the S_1 origins for ethylbenzene and ethylbenzene–Ar. In the bare ethylbenzene, its rotational contour exhibits a typical pattern attributable to the perpendicular electronic transition of a symmetric top molecule. This ob-

Table 1
Rotational constants of ethylbenzene–Ar (isomers A and B) and ethylbenzene, obtained from the optimized structure by the MP2/3-21+G** calculation (The moment of inertia are indicated by *A*, *B*, and *C*, and the asymmetric parameter by *K*)

	Rotational constants (cm^{-1})			
	A	*B*	*C*	*K*
Ethylbenzene	0.151	0.0484	0.0406	−0.859
Ethylbenzene–Ar (A)	0.0409	0.0398	0.0259	0.853
Ethylbenzene–Ar (B)	0.0474	0.0308	0.0235	−0.389

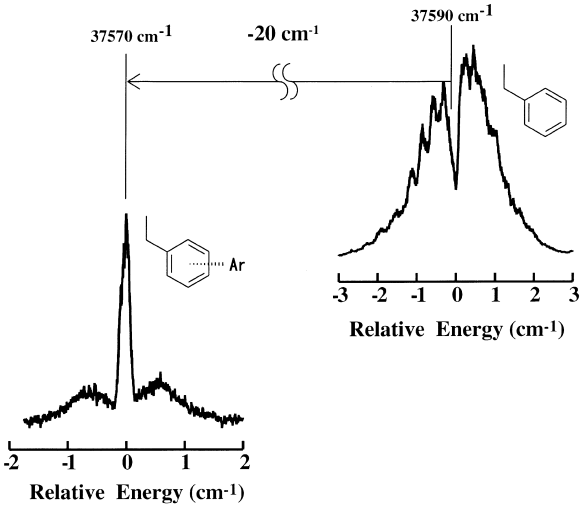

Fig. 4. TOF-MPI excitation spectra observed for ethylbenzene–Ar and the bare ethylbenzene, which are due to their $S_1 \leftarrow S_0$ (0_0^0) transitions.

servation is reasonably explained, since the direction (C axis) of the principal moment of inertia obtained from the calculations is along the phenyl–ethyl axis, while the electronic transition moment of $S_1 \leftarrow S_0$ lies in the phenyl plane and is perpendicular to the phenyl–ethyl axis. The rotational contour of ethylbenzene–Ar, on the other hand, exhibits a typical pattern attributable to the parallel electronic transition of a symmetric top molecule. If this complex takes the form of isomer A, the experimental result is also reasonably explained for the following reasons. (1) The isomer A is a symmetric top ($\kappa = 0.853$). Its calculated principal moment of inertia is in the direction (C axis) parallel to the electronic transition moment; that is, in the direction perpendicular to the phenyl–ethyl axis in the phenyl plane. (2) The isomer B is apparently asymmetric ($\kappa = -0.389$). From these calculations and the rotational contour spectrum, the isomer we have measured may be safely assigned to the isomer A. The form of A may also be assumed for the n-propylbenzene–Ar vdW complex.

The shifts in the S_1 origins have been found to be 20 and 21 cm^{-1} for ethylbenzene–Ar and n-propylbenzene–Ar, respectively, with respect to their bare molecules. It is noted that the observed shift is for the *trans* form of n-propylbenzene. The n-propylbenzene molecule (phenyl–$C_\alpha H_2$–$C_\beta H_2$–CH_3) is known to have the two conformers (*trans* and *gauche*) around the C_α–C_β bond [35,36]. The S_1 origins thus determined were selected as intermediate resonant states during the (1+1′) ZEKE experiments. For *gauche* n-propylbenzene it was difficult to find an appreciable MPI peak due to its Ar complex, though an MPI peak due to the bare molecule can be observed, as reported in the previous study [36].

3.3. ZEKE electron spectra

Fig. 5 shows ZEKE electron spectra observed for the series of the vdW complexes (benzene–Ar, toluene–Ar, ethylbenzene–Ar, and n-propylbenzene–Ar) in the low-energy region at the cation ground state. The horizontal axis shows the energy shifts from the free alkylbenzenes. The D_0 origins of ethylbenzene–Ar and n-propylbenzene–Ar (*trans*)

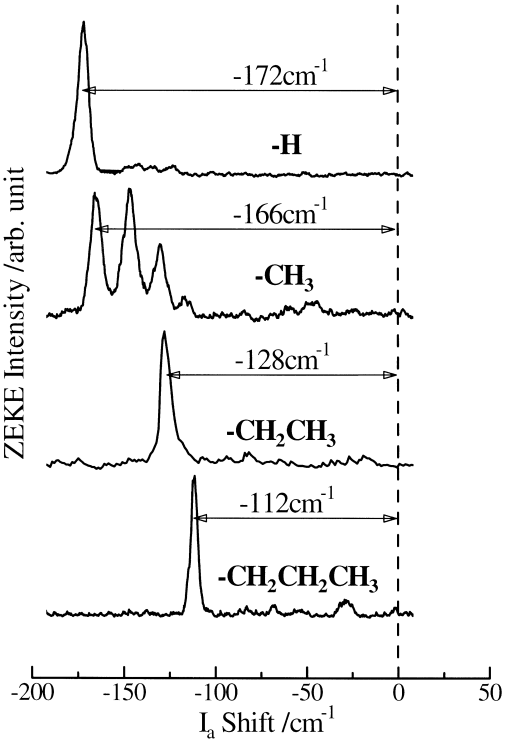

Fig. 5. ZEKE electron spectra observed in the low-energy region for benzene–Ar and the three alkylbenzene–Ar complexes (toluene–Ar, ethylbenzene–Ar, and *trans* n-propylbenzene–Ar), illustrated with respect to the I_a shifts.

Table 2
Adiabatic ionization energies (I_a) of ethylbenzene–Ar and *trans* n-propylbenzene–Ar, and their shifts with respect to their bare molecules

Molecular species	I_a (cm^{-1})	ΔI_a (cm^{-1})
Ethylbenzene–Ar	70 634±6	−128
Ethylbenzene	70 762±6	
trans n-Propylbenzene–Ar	70 160±6	−112
trans n-Propylbenzene	70 272±6	

are summarized in Table 2, which were determined in the present study for the first time from the ZEKE electron spectra. The D_0 origins observed for benzene–Ar and toluene–Ar are essentially the same as those reported previously [6,25].

3.4. vdW vibration of benzene–Ar

In addition to the cation origin peak (0^{+0}) of benzene–Ar, Fig. 6 shows several ZEKE electron bands due to vdW vibrations at 24, 29, 38, and 48 cm^{-1} in the low-energy region, which have been observed for the first time in the present study. These observed vibrational frequencies are summarized in Table 3, together with their possible spectral assignments. The benzene–Ar cation has a total of three vdW vibrational modes, which may be represented as totally symmetric bending mode (b_x^+), non-totally symmetric bending mode (b_y^+) and stretching mode (s_z^+). Here, *z* is the axis perpendicular to *x* and *y*.

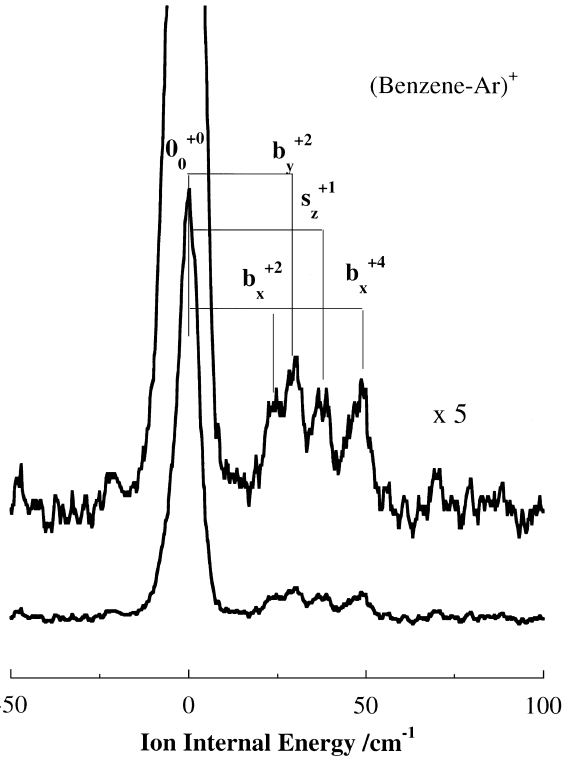

Fig. 6. The ZEKE electron spectrum of benzene–Ar is shown in an expanded scale, consisting of several weak bands attributable to vdW vibrations in addition to the main cation band (0^{+0}).

A vibrational progression due to the toluene–Ar cation is clearly shown with a spacing of 17 cm^{-1} in Fig. 5, essentially the same as that previously observed and assigned to the bending mode (b_x^+) by Inoue et al. [25]. This frequency of the vdW bending is similar to those reported for other aromatic–Ar vdW cations; for example, 16 cm^{-1} for (aniline–Ar)$^+$ [13], 12 cm^{-1} for (benzonitrile–Ar)$^+$ [20], 12 cm^{-1} for (fluorobenzene–Ar)$^+$ [24].

The four bands appearing at 24, 29, 38, and 48 cm^{-1} in the ZEKE electron spectrum due to the benzene–Ar cation have been tentatively assigned as b_x^{+2}, b_y^{+2}, s_z^{+1}, and b_x^{+4}, respectively, as summarized in Table 3. Therefore it may be indicated that the vibrational frequencies of the three kinds of vdW vibrations of the benzene–Ar cation are12 cm^{-1} (b_x^+), 15 cm^{-1} (b_y^+), and 38 cm^{-1} (s_z^+ mode). It should be mentioned that the cation vdW bending can be observed for benzene–Ar (Fig. 6) and toluene–Ar (Fig. 5), but not for ethylbenzene–Ar and n-propylbenzene–Ar (*gauche*).

The absence of the cation vdW bending for ethylbenzene–Ar and n-propylbenzene–Ar may be explained by considering steric hindrance between the Ar atom and the alkyl group, as described in the later section. The overtones of vdW bending vibration of benzene–Ar were observed with very weak intensities (Fig. 6), since the vdW bending vibration of benzene–Ar is non-totally symmetric under C_{6v} symmetry.

Table 3
ZEKE electron bands observed for benzene–Ar in the low-energy region, and their possible assignments to vdW vibrations

	Ion internal energy (cm^{-1})				
	0 (74 385)	24	29	38	48
Assignment	0^{+0}	b_x^{+2}	b_y^{+2}	s_z^{+1}	b_x^{+4}

3.5. Lennard–Jones (LJ) potential analysis of vdW interactions

In order to obtain information about the stable structure and the vdW forces in alkylbenzene–Ar, we carried out theoretical calculations of potential energy curves as a function of the distance between the Ar atom and the C and H atoms of the alkylbenzene moiety by using the atom–atom LJ potential. Charge-induced dipole interactions were taken into account to explain the vdW interactions in the vdW cations. Calculations of the molecular structure and the atomic charge distributions of the alkylbenzene moiety were carried out at the neutral S_0 and cation D_0 states, using the density functional ab initio calculations.

The vdW potential energy between Ar and the alkylbenzene may be given by:

$$V(r_{Ar-Ci}, r_{Ar-Hj}) = \sum_i V_{Ar-C}(r_{Ar-Ci}) + \sum_j V_{Ar-H}(r_{Ar-Hj}) + \sum_{i,j} V_e(r_{Ar-Ci}, r_{Ar-Hj}) \quad (1)$$

where r_{Ar-Ci} is the distance between Ar and the ith C atom of the alkylbenzene moiety, and r_{Ar-Hj} is the distance between Ar and the jth H atom. As indicated by Leutwyler and Jortner [29] in their LJ potential analysis of intermolecular interaction, the first term is the total potential energy between the Ar and the C atoms, given by:

$$V_{Ar-C}(r_{Ar-Ci}) = 4\epsilon_{Ar-C}\{(\sigma_{Ar-C}/r_{Ar-Ci})^{12} - (\sigma_{Ar-C}/r_{Ar-Ci})^{6}\} \quad (2)$$

and the second term is the total energy between the Ar and the H atoms, given by:

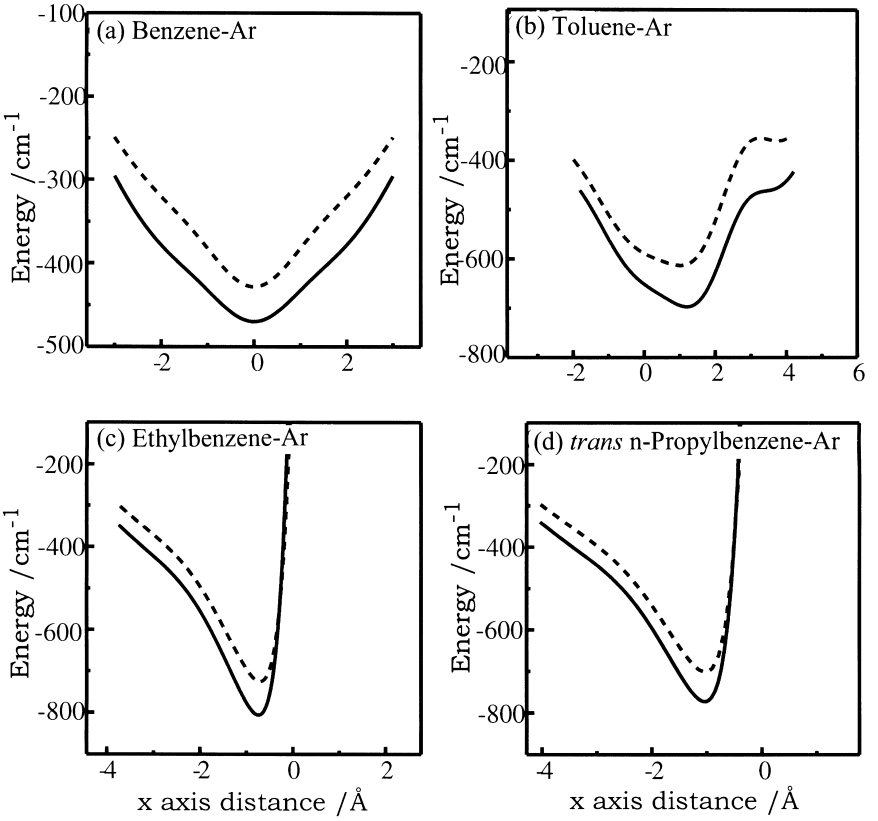

Fig. 7. Lennard–Jones potentials obtained from the theoretical calculations for the series of the vdW complexes at the neutral ground state S_0 (broken line) and the cation ground state D_0 (solid line): (a) benzene–Ar, (b) toluene–Ar, (c) ethylbenzene–Ar, and (d) n-propylbenzene–Ar.

$$V_{Ar-H}(r_{Ar-Hj}) = 4\epsilon_{Ar-H}\{(\sigma_{Ar-H}/r_{Ar-Hj})^{12} - (\sigma_{Ar-H}/r_{Ar-Hj})^{6}\} \quad (3)$$

where ϵ_{Ar-C}, ϵ_{Ar-H}, σ_{Ar-C} and σ_{Ar-H} are the usual potential parameters. For these parameters the same values were used as those reported for naphthalene–Ar by Mandziuk and Bacic [37]: $\epsilon_{Ar-C} = 40.05\ cm^{-1}$, $\epsilon_{Ar-H} = 17.94\ cm^{-1}$, $\sigma_{Ar-C} = 3.385$ Å, $\sigma_{Ar-H} = 3.207$ Å. The first two terms are essentially the same as those reported by Leutwyler and Jortner [29]. The third term is the 'charge-induced dipole interaction' expressed by:

$$V_e(r_{Ar-Ci}, r_{Ar-Hj}) = -(1/2)\{Q_{Ci}^2\chi_{Ar}/r_{Ar-Ci}^4 + Q_{Hj}^2\chi_{Ar}/r_{Ar-Hj}^4\} \quad (4)$$

where Q_{Ci} and Q_{Hj} represent charges at the ith C atom and the jth H atom, respectively, and χ_{Ar} is the polarizability of Ar. The charges on the C and H atoms were obtained from the ab initio MO calculations with B3LYP/6-31G*. A value of 1.650 $Å^3$ was used for χ_{Ar}. Any interaction caused by a positive charge deposited on the Ar atom was neglected in these calculations.

The potential energy curves calculated along the x axis (the long axis of the phenyl group) are shown in Fig. 7, for benzene–Ar, toluene–Ar, ethylbenzene–Ar, and n-propylbenzene–Ar. The potential energy curve of benzene–Ar is symmetric with respect to the origin, and there is no shift in the potential minimum between the neutral and the cationic state, as shown in Fig. 7a. However, the potential energy curves are asymmetric for toluene–Ar, ethylbenzene–Ar and n-propylbenzene–Ar (Fig. 7). The potential energy minimum of toluene–Ar is shifted by 0.17 Å between the neutral and the cationic state, while the corresponding shift is 0.03 Å for ethylbenzene–Ar and it is less than 0.01 Å for n-propylbenzene–Ar. The shift of the Ar atom in the relative position is rather restricted by the alky substituent for both ethylbenzene–Ar and n-propylbenzene–Ar in the A-type form (Fig. 3), in constant to toluene–Ar. If the B-type form (Fig. 3) is assumed for ethylbenzene–Ar and n-propylbenzene–Ar, their LJ potential curves would be much similar to that of toluene–Ar. These calculations are consistent with the present experimental results that no vdW progress appears in the ZEKE electron spectra for ethylbenzene–Ar and n-propylbenzene–Ar, as seen from Fig. 5.

3.6. Dissociation energies

The shift in ionization potential, ΔI_a, can be expressed in terms of the dissociation energies of alkylbenzene–Ar at the neutral S_0 and cation D_0 states by the relationship:

$$\Delta I_a = I_a(\text{alkylbenzene–Ar}) - I_a(\text{alkylbenzene}) = D_0'' - D_0^+ \quad (5)$$

where D_0'' and D_0^+ are the dissociation energies of alkylbenzene–Ar at the S_0 and D_0 states, respectively. The experimental values of ΔI_a are plotted against the alkyl groups (–H, $-CH_3$, $-C_2H_5$, and $-C_3H_7$) in Fig. 8, compared with the difference $(D_0'' - D_0^+)$ deduced from the calculations of the LJ potential energies 'with' and 'without' considering the atomic charge distribution at the neutral S_0 state. It is

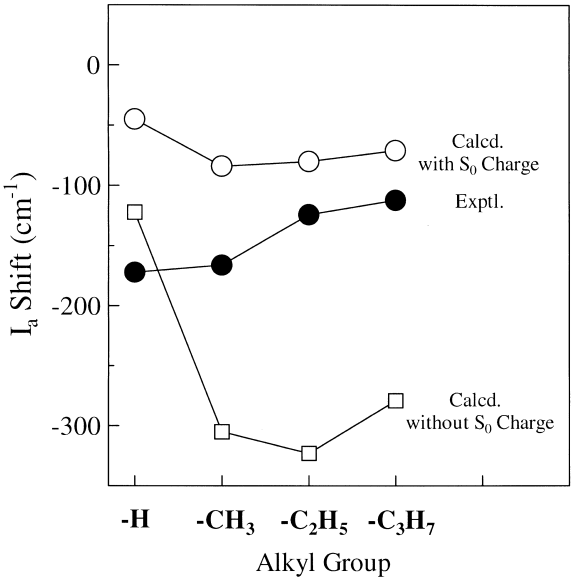

Fig. 8. The experimental I_a shifts (black circles) plotted against the order of the alkyl groups are compared with the corresponding theoretical values, which were obtained with and without including atomic charge distributions (open circles and squares, respectively) at the neutral S_0 state. Here, the atomic charge distributions were obtained from the ab initio B3LYP/6-31G* calculations.

evident that the atomic charge distributions should be taken into account even at the S_0 states.

4. Conclusions

In the present work, the ZEKE electron spectra of ethylbenzene–Ar and n-propylbenzene–Ar (*trans*) have been observed for the first time. The ethylbenzene–Ar vdW complex has been confirmed to be mainly attributable to isomer A (Fig. 3) from our TOF-MPI and ZEKE spectra and also from our LJ potential energy analysis. For these alkylbenzene–Ar complexes, the stabilization in the dissociation energy of the vdW complex cation with respect to the neutral vdW complex has been reasonably explained in terms of the charge–charge-induced-dipole interaction model.

References

[1] K. Kimura, in: C.-Y. Ng (Ed.), Photoionization and Photodetachment, World Scientific, Singapore, 1999.
[2] K. Kimura, Adv. Chem. Phys. 60 (1985) 161.
[3] K. Kimura, Int. Rev. Phys. Chem. 6 (1987) 195.
[4] K. Sato, Y. Achiba, K. Kimura, J. Chem. Phys. 81 (1984) 57.
[5] K. Müller-Dethlefs, M. Sander, E.W. Schlag, Chem. Phys. Lett. 112 (1984) 291.
[6] L.A. Chewter, K. Müller-Dethlefs, E.W. Schlag, Chem. Phys. Lett. 135 (1987) 219.
[7] K. Müller-Dethlefs, E.W. Schlag, Annu. Rev. Phys. Chem. 42 (1991) 109.
[8] Y. Achiba, K. Sato, K. Kimura, in: Second Symposium of Chemical Reaction, Abstract, The Chemical Society of Japan, 1985, p. 24, in Japanese.
[9] M. Takahashi, K. Okuyama, K. Kimura, J. Mol. Struct. 249 (1991) 47.
[10] M. Takahashi, H. Ozeki, K. Kimura, Chem. Phys. Lett. 187 (1991) 250.
[11] K. Kimura, M. Takahshi, in: C.-Y. Ng (Ed.), Optical Methods for Time- and State-Resolved Chemistry, Vol. 163, SPIE: The International Society for Optical Engineering, Bellingham, WA, 1992, p. 6.
[12] M. Takahashi, J. Chem. Phys. 96 (1992) 2594.
[13] M. Takahashi, H. Ozeki, K. Kimura, J. Chem. Phys. 96 (1992) 6399.
[14] S. Sato, K. Kimura, Chem. Phys. Lett. 249 (1996) 155.
[15] X. Zhang, J.M. Smith, J.L. Knee, J. Chem. Phys. 97 (1992) 2843.
[16] M.C.R. Cockett, K. Okuyama, K. Kimura, J. Chem. Phys. 97 (1992) 4679.
[17] J.M. Dyke, H. Ozeki, M. Takahashi, M.C.R. Cockett, K. Kimura, J. Chem. Phys. 97 (1992) 8926.
[18] K.-T. Lu, G.C. Eiden, J.C. Weisshaar, J. Phys. Chem. 96 (1992) 9742.
[19] M.C.R. Cockett, K. Kimura, J. Chem. Phys. 100 (1994) 3429.
[20] M. Araki, S. Sato, K. Kimura, J. Phys. Chem. 100 (1996) 10542.
[21] T. Vondrak, S. Sato, K. Kimura, Chem. Phys. Lett. 261 (1996) 481.
[22] T. Vondrak, S. Sato, K. Kimura, J. Phys. Chem. A 101 (1997) 2384.
[23] T. Vondrak, S. Sato, V. Spirko, K. Kimura, J. Phys. Chem. A 101 (1997) 8631.
[24] H. Shinohara, S. Sato, K. Kimura, J. Phys. Chem. A 101 (1997) 6736.
[25] H. Inoue, S. Sato, K. Kimura, J. Electron Spectrosc. 88–91 (1998) 125.
[26] S. Sato, K. Omiya, K. Kimura, J. Electron Spectrosc. 97 (1998) 121.
[27] D. Tanaka, S. Sato, K. Kimura, Chem. Phys. 239 (1998) 437.
[28] J.B. Hopkins, D.E. Powers, R.E. Smalley, J. Chem. Phys. 72 (1980) 5039.
[29] S. Leutwyler, J. Jortner, J. Phys. Chem. 91 (1987) 5558.
[30] K. Kimura, J. Electron Spectrosc. Relat. Phenom. 100 (1999) 273.
[31] W. Caminati, D. Damani, G. Gorbelli, B. Velino, C.W. Bock, Mol. Phys. 74 (1991) 885.
[32] J.B. Lagowski, I.G. Csizmadia, G.J. Vancso, J. Mol. Phys. 258 (1992) 341.
[33] A.D. Becke, J. Chem. Phys. 98 (1993) 5648.
[34] M.J. Frisch, G.W. Trucks, H.B. Schlegel, P.M.W. Gill, B.G. Johnson, M.A. Robb et al. (Eds.), Gaussian 94, Revision C.3, Gaussian Inc, Pittsburgh, PA, 1995.
[35] X. Song, C.W. Wilkerson Jr., J. Lucia, S. Pauls, J.P. Reilly, Chem. Phys. Lett. 174 (1990) 377.
[36] M. Takahashi, K. Kimura, J. Chem. Phys. 97 (1992) 2920.
[37] M. Mandzuik, Z. Bacic, J. Chem. Phys. 98 (1993) 7165.